RSC Advances

ROYAL SOCIETY OF CHEMISTRY

www.rsc.org/advances

Continuous Catalytic Upgrading of Fast Pyrolysis Oil Using Iron Oxides in Red Mud

James R. Kastner*[1], Roger Hilten[1], Justin Weber[1], Andrew R. McFarlane[2], Justin S.J. Hargreaves[2], Vidya S. Batra[3]

[1]Biochemical Engineering, College of Engineering
The University of Georgia, Athens GA 30602, USA
*Corresponding author phone: 706-583-0155; fax: 706-542-8806

e-mail: jkastner@engr.uga.edu

[2]University of Glasgow (UG), Justin.Hargreaves@glasgow.ac.uk

[3]The Energy and Resources Institute (TERI, India), vidyasb@teri.res.in

Abstract

A catalyst composed of primarily magnetite was prepared from red mud, via H_2 reduction at 300°C, which significantly increased surface area. Ammonia and CO_2 temperature programmed desorption indicated both acid and base active sites. Continuous reaction studies conducted with individual, mixtures of model compounds, and water extracted fast pyrolysis oil indicated acetone was the primary product from acetic acid, and acetone and 2-butanone from acetol. Levoglucosan entered the same pathway, since it formed acetic, formic, and acetol. Total conversion and yields approached 100% and 22 mol% ketones at 400°C and a W/F of 6 h for a model mixture and 15-20 mol% ketones at W/F 1.4-4 h and 400-425°C using water extracted oil. Space time yields approached 60 g ketones/L-cat/h for the model mixture and 120 g/L-cat/h for a commercial oil. The catalyst simultaneously reduced acidity, recovered carbon, and generated upgradable intermediates from the aqueous fraction of fast pyrolysis oil in a "continuous" process.

Index Words: Red Mud; Catalyst; Continuous; Ketonization; Levoglucosan

1. Introduction

Biomass fast pyrolysis is a rapid thermal process (0.5-5 seconds compared to days for biochemical conversion) that generates an energy dense, oxygenated liquid hydrocarbon stream in high yields (60-75%) that in theory can be catalytically converted to drop-in biofuels. [1,2] However, due to the presence of water (30-40%), reactive acids and aldehydes, as well as tars, the resulting oil is acidic (corrosive), unstable (polymerization reactions increase viscosity), and difficult to catalytically upgrade to a drop-in biofuel.[3]

Since fast pyrolysis oil (FPO) is unstable, much effort has focused on stabilizing the oil for storage and shipment to bio/refineries, including techniques such as solvent addition, catalytic esterification, mild catalytic hydrodeoxygenation, and acid-catalyzed cracking.[3-7] Solvent addition and esterification require methanol or ethanol addition.[8] Catalytic decarboxylation (CO_2 loss) and decarbonylation (CO loss) of the acids and aldehydes have been proposed to deoxygenate and stabilize the oil for further treatment. However, these processes produce lower molecular weight products without the formation liquid fuel intermediates. Catalytic upgrading of pyrolysis oils using current acid catalysts (e.g., zeolites, such as H-ZSM-5) and FCC catalysts is not sustainable due to coke formation and catalyst deactivation.[6,7]

Instead of breaking the acids in the oil down to only CO and CO_2, it has been proposed to reduce the oxygen content and acidity of the bio-oil by combining these molecules via catalytic ketonization, condensation, and deoxygenation reactions. A range of metal oxides have been reported to perform these reactions including iron oxides supported on SiO_2, TiO_2 and Al_2O_3. [9,10] Alternative to expensive catalysts that ultimately deactivate/coke and have to be recovered and re-synthesized, it has recently been demonstrated that it is possible to catalytically upgrade fast pyrolysis oil using solid catalysts synthesized from red mud.[11-14] Red mud contains many

potentially active metal oxides including, SiO_2 [2-22%], Al_2O_3, [8-48%], Fe_2O_3 [12-60%], TiO_2, [5-20%], CaO, [4-46%], and MgO, [0.2-2%][15,16] and is inexpensive, compared to the high cost of Pd (>$10,000/kg), Pt (>$10,000/kg), Ru (~$5,000/kg), Ce ($300-400/kg), Zr ($250/kg), and Ti ($10/kg) [Pd, Pt, and Ru costs were estimated from the literature[17] and Ce, Zr, and Ti costs were estimated at usgs.gov (1998)]. The contribution of metal cost to supported catalyst prices range from $9-10/kg for CoMo, $70-100/kg to $1000/kg for 1 wt.% Ru to Pt respectively, $500-10,000/kg for 5-20 wt.% Ru to Pt on carbon catalysts respectively, and $1000-50,000/kg for bulk catalysts of Ru to Pt respectively.[17] The added advantage of using red mud is that the spent catalyst can be reused for another purpose. For example, the spent coked catalyst (red mud) could be gasified to generate hydrogen (iron is a good gasification catalyst), used as coke in iron making, or used to remove tar from syngas streams.[18,19]

Recent research indicates that activated red mud (H_2 reduced) can catalytically ketonize a wide range of carboxylic acids in aqueous solutions.[12,13] The primary products of these reactions were longer chain alkenes and ketones. Thus, the feasibility of using red mud as a catalyst to upgrade fast pyrolysis oil has been established via batch reactions, yet the practicality and knowledge base for its use in a continuous industrial process remains to be demonstrated and developed. Transformation studies on acetic and formic acid and whole oil using red mud have been conducted,[11-14] yet there has been little research on other key components in fast pyrolysis (e.g., acetol and levoglucosan). Previous work has been conducted in batch reactors at high pressure (350-365°C, 3,000-4,000 psi) and long residence times (4-8 h). Batch reactors are inherently non-steady state thus leading to difficulties in accurately measuring reaction rates, product yields, selectivity, and space time yields. The development of continuous routes, especially if operational at lower pressures and residence times, would be of great interest. To

date, there has been very little research investigating "continuous" catalytic ketonization and deoxygenation of fast pyrolysis oil using catalysts derived from red mud reported. Such studies would enable accurate measurement of reaction rates, space time yields, selectivity, and catalyst longevity.

One option to catalytically upgrade FPO is to couple a phase separation process that reduces the complexity, viscosity, and cross reactions in the bio-oil, with a catalytic process that reduces H_2 consumption and conserves carbon, while forming hydrocarbons.[20, 21] Using this approach, Zhao and Lercher (2012) performed batch, catalytic hydrodeoxygenation of hexane extracted bio-oil, containing primarily substituted phenols, using Ni/HZSM-5 (532K, 5 MPa, H_2) to generate C_5-C_9 hydrocarbons.[21] Other than aqueous phase reforming (APR), limited research has focused on the catalytic conversion of the aqueous phase derived from fast pyrolysis oil. Water addition to fast pyrolysis oil generates a two phase system (oil and water) that extracts the carbohydrates, aldehyes, ketones, and acids into the aqueous phase enabling easier catalytic upgrading. For example, fast pyrolysis oil generated from pine contacted with water at 34°C for 15 minutes generated an aqueous phase with 78 g/L of levoglucosan and estimated acetic and formic acids levels of 28 and 20 g/L respectively (final total water content of 62%).[22] More detailed water extraction studies indicate that water to oil ratios as low as 0.5 (20°C, 300 rpm, 24 h) can result in yields from 80-90% for levoglucosan, glycoaldehyde, acetol, and acetic acid from pine bio-oil.[23]

Thus, the goal of this research was to determine the feasibility of "continuous" catalytic ketonization of an aqueous extract of fast pyrolysis oil (FPO) using red mud, acquire knowledge of active sites in red mud responsible for these reactions, and begin to understand reaction pathways in the mixed reactant environment of fast pyrolysis oil. Given the complexity of fast

pyrolysis oil, the high level of water, and the propensity to polymerize upon heating, we selected to work with representative model compounds in an aqueous phase and water extracted FPO.

2. Material and methods

2.1 Catalyst Preparation. A sample of red mud was obtained from Rio Tinto (Alcan, Canada), dried (105°C), crushed into granules, sieved into two size fractions, and reduced using H_2 (50-65 g of red mud reduced in-situ under flowing H_2 [100%] at 90 mL/min by heating at 10°C/min to 300°C and holding for 20 h. The reduced fraction (1.5-2 mm) was used in a packed bed reactor to treat model compounds and fast pyrolysis oil.

2.2 Catalyst Characterization. Surface areas of the solid acid catalysts (0.1 g sample size) were measured by N_2 adsorption over a relative pressure range (P/P_0) of 0.05–0.35 using a 7-point Brunauer-Emmet-Teller (BET) analysis equation (Quantachrome AUTOSORB-1C; Boynton Beach, FL). Pore size distribution, average pore radius, and total pore volume were estimated from N_2 desorption curves using the Barrett, Joyner and Halenda method (BJH). All samples were degassed ranging from 250 to 300°C for 3–4 h before analysis. Compositional analysis of the red mud and derived catalysts was performed using ICP-MS in scan mode (samples were digested utilizing nitric and hydrofloric acid in sealed teflon containers in a microwave at 400W for 25 min).

Powder XRD patterns were recorded with a Siemens D5000 Diffractometer using Cu-Kα radiation. Samples were prepared by compaction into sample holders and measurements were undertaken in the 5-85 º 2θ range with a step size of 0.02º using a counting rate of 1s per step.

Red mud (dried, crushed and sieved), unreacted catalyst (reduced red mud), and reacted catalyst were analyzed by H_2-TPR and NH_3-CO_2-TPD. Ammonia temperature programmed

desorption (TPD) was used to estimate acid site strength of the catalysts. All samples were degassed ranging from 250 to 300°C for 3–4 h before NH_3 or CO_2 TPD analysis. Samples (0.2 g) were loaded in a quartz U-tube and packed between two quartz-wool layers, degassed at 185°C for 30 min in helium, saturated with ammonia (pure electronic grade) at 40°C for 15 min, flushed with helium at 40°C for 15 min, then desorbed with helium from 40 to 800°C at 10°C/min (all flows at 80 mL/min). For CO_2-TPD, samples were saturated with 100% CO_2 at 30°C for 10 min, then desorbed with helium from 30 to 800°C at 10°C/min (all flows at 80 mL/min). Desorbed NH_3 and CO_2 were detected using a TCD (16×attenuation) and measurements were made using a Quantachrome AUTOSORB-1C instrument.

Hydrogen temperature programmed reduction (TPR) was used to estimate the iron valance state in the red mud catalyst and reacted catalysts. Degassed samples (0.2 g) were loaded in a quartz U-tube and packed between two quartz-wool layers, degassed at 185°C for 30 min in N_2, the temperature reduced to 60°C and switched to H_2 (4% in N_2) flow while heating to 800°C at 20°C/min. The reduction in H_2 concentration across the catalyst was monitored using a TCD.

Recovered catalysts were washed with an equal volume mixture of toluene, acetone, and methanol to remove tar. Approximately 2 g of reacted catalyst was placed on a Whatman Filter (Qualitative #1 Filter Paper, 70 mm) and rinsed under vacuum with the solvent mixture. The rinsed catalyst was then dried at 105 °C for 1 hour, cooled to room temperature, and weighed to determine the mass of tar/coke accumulated. Catalyst coke formation was determined by heating the washed catalyst in a thermogravimetric analyzer (TGA) at 10 °C/min to 800 °C under air flow. The change in the mass of catalyst was assumed to be due to the complete combustion of coke.

2.3 Analytical. Chemical composition of the fast pyrolysis oil and the upgraded samples was determined by GC-MS analysis using a Hewlett-Packard (Model HP-6890) gas chromatograph in conjunction with a Hewlett-Packard mass spectrometer (Model HP-5973) with a mass selective detector. The GC contained an HP-5 MS column of the following dimensions: 30 m length, 0.25 mm internal diameter, and 0.25 μm film thickness. The method used was as follows: inlet temperature 240˚C, detector temperature 280˚C (mass spectrometer interface temperature), flow at 1 mL min^{-1} He, oven at 40˚C for 3 min followed by a ramp at 8˚C min^{-1} to 250˚C (held for 5 min). The mass spectrometer scan range was from 20-350 mass units. A sample size of 1 µL was used and samples were prepared for GC-MS analysis by diluting the fast pyrolysis oil to 2.5 % (v/v) with acetone. The compounds were identified using Agilent Technologies software (MSD ChemStation D.03.00.611), which uses a probability-based matching (PBM) algorithm to match unknown spectra to those found in a mass spectral library using National Institute of Standards and Technology's 2008 version (NIST 2008). The quality of a match determined by ChemStation is defined as the probability that the unknown is correctly identified as the reference. Match quality ranges between 1 and 100 and values above 90 were considered as very good matches in our analysis.

In some cases the fast pyrolysis oil and catalytically upgraded oil were quantitatively analyzed using an external standard and GC/MS analysis. Hexanol was used as the standard and added to the oil at 2.03 g/L and analyzed using the previously described methods. Neat compounds of 1-hydroxy-2-propanone, furfural, 2-methoxy phenol, 2-methoxy-4-methyl phenol, tetrahydrofuran, 2-butanone, 1-butanol, and eugenol (99.9%, Sigma) were mixed with hexanol (2.03 g/L), acetone, and methanol to generate standard mixtures and analyzed on the GC/MS using identical methods.

Identification of products in the condensed liquid outlet was based on GC/MS matching with a NIST database and then retention time matching using purchased standards on the GC/MS using the HP-5 column and on the Innowax column using a separate GC/FID. The compounds identified in this manner were acetone, 2-butanone, furfural, and butyrolactone. For other intermediates and products identified by GC/MS that could not be purchased, we report match factors with the NIST database for these compounds. Two match factors are reported, a reverse search ignoring peaks in the unknown not in the library spectrum (RMatch) and a probability value (Prob.%). The probability value assumes the unknown is represented by a spectrum in the library and employs the differences between adjacent hits in the hit list to get the relative probability that any hit in the hit lists is correct. In general according to NIST, 900 or greater is an excellent match; 800–900, a good match; 700–800, a fair match. Less than 600 is a very poor match.

The water soluble components in the oil were analyzed by a high performance liquid chromatography (LC-20 AT, Shimadzu Corp., USA) equipped with a RID-10A refractive index detector and a 7.8×300 mm Coregel 64-H transgenomic analytical column for sugars (e.g., levoglucosan) and carboxylic acids (e.g., formate and acetate). About 2 mL of the oil was diluted with DI water at 1:1 ratio and centrifuged at 5000 rpm for 30 min, and then decanted. The supernatant was filtered through a 0.45-μm filter into 2-mL auto-sampling vials. A sample size of 5 μL was injected into the column using the LC-20 AT Shimadzu auto-injector. The samples were analyzed at 6.89 MPa (1000 psi) and 60˚C with an eluent (4 mN H_2SO_4) flow rate of 0.6 mL min^{-1} for a 55 min run time. Glucose and xylose (if present), formic acid, acetic acid, levoglucosan, cellobiosan (if present), furfural, hydroxyl methyl furfural (HMF), and sorbitol (if

present) in the liquid samples were identified by comparing retention times with standards and quantified using a 5 point standard curve.

2.4 Feedstock Preparation. In this work a series of experiments have been performed in which individual model compounds (4 wt.% each in water: acetic, formic, 1-hydroxy-2-propanone or acetol, and levoglucosan), mixtures of the model compounds, and water extracted fast pyrolysis oil were catalytically transformed using reduced red mud (RRM, typically 1-2 h runs). The feed and condensed products were analyzed via GC/MS, GC/FID, and HPLC. The water extracted fast pyrolysis oil was generated using two methods from two types of oil.

Fast pyrolysis oil (FPO) was generated from Southern Pine as previously described,[8] and a commercially produced hardwood FPO was secured. Both oils were stored at 4°C and analyzed before use to verify inlet concentrations (note, the aqueous model compounds and mixtures were also subsampled and analyzed via GC/FID and HPLC). Water extracted oil (WE-FPO) was prepared by two methods – 1:1 (oil:water v/v) mixing at room temperature, followed by centrifugation at 5,000 rpm for 15 min and decanting the aqueous top phase (phase used in catalytic upgrading experiments), and in-line condensation. The in-line condensation process to form two phases was performed by contacting atomized water vapor with fast pyrolysis bio-oil vapor/aerosol as it was formed. Fast pyrolysis of pine pellets was conducted at 500°C in an auger fed fluidized bed reactor where bed material and biomass was fluidized using N_2 (20 L/min) and controlled using a thermal mass flow controller. Water vapor was added (79-102 g/hr) via a small bore atomizer upstream from the condenser to generate an ~1:1 wt % water to oil condensate, which phase separated. The oil feed rate to the in-line condensation process (ILC) was 40-147 g/hr and phase separated when collected in a temperature controlled shell and tube condenser using a circulating ice water bath.

2.5 Reaction Kinetics. Model compounds, their mixtures, and phase separated bio-oil was injected continuously (downward) using an HPLC pump into a packed bed reactor or PBR (Parr Moline, IL) maintained at 350, 375, 400, or 425 °C in a tube furnace (Thermocraft Lab-Temp 1760-watt tube furnace). The PBR consisted of a 2.4 cm inner diameter reactor with a 38 cm length. A 15 cm preheater section was incorporated into the reactor to ensure that bio-oil was in vapor phase prior to crossing the catalyst bed (5 [2.3], 10 [4.3], 15[6.9], and 20 [9.2] g catalyst [packing height cm], 0.941 g/ml bulk density) that was held in place by stainless-steel screens and quartz wool above and below the bed. Liquid feed was typically 1.0 cm^3 min^{-1}, corresponding to a catalyst mass to feed ratio (W/F) ranging from 0.7-6.0 h (g cat/g feed $^{-1}$ h^{-1}). The liquid feed was mixed with an inert gas (N_2) which had flow rate of 100 cm^3 min^{-1} (controlled using mass flow controllers - Brooks Delta II Smart). Weight hourly space velocity (WHSV) was calculated as the mass flow rate (g h^{-1}) of liquid feed divided by the catalyst mass (g) and ranged from 0.18-1.44 g feed g cat^{-1} h^{-1} . These reaction conditions corresponded to a liquid hourly space velocity [LHSV = reactant liquid flow rate (cm^3 h^{-1})/reactor volume (cm^3)] ranging from 1.4-11.3 h^{-1}. Given a carrier gas flow rate of 100 cm^3 min^{-1}, gas-phase residence time in the catalytic zone (H = 1-4 cm) ranged from approximately 3-13 s. The outlet gas passed through custom designed condenser vessel (Parr) and chilled using a Brookfield TC-602 water bath.

3. Results and Discussion

3.1 Catalyst Characterization. Elemental analysis indicated high levels of Fe, Al, Si, and Na, with lower levels of Ca, K, and Ti typical of red mud and little change upon H_2 reduction at 300°C (Table 1). Hydrogen reduction of red mud at 300°C increased the surface area by 57%

and average pore size by 11% (Table 1). The increase in pore size was most noticeable in a plot of pore size distribution indicating a significance increase in pores of radius 18-19 Å (Fig. 1SD). Similarly, XRD analysis also indicated a significant change in structure upon H_2 reduction. The granulated red mud was composed primarily of hematite with some XRD signals indicating the presence of rutile. Upon H_2 reduction, reflections corresponding to the presence of magnetite were apparent in the H_2 reduced red mud (Fig. 2SD). The formation of magnetite was also corroborated by H_2-TPR. Analysis indicated a peak in H_2 consumption around 600°C and a smaller amount of H_2 consumption for the reduced red mud, suggesting that a portion of the hematite (Fe_2O_3) in our original material was reduced to magnetite (Fe_3O_4 – Fig. 3SD). Ammonia and CO_2 TPD analysis of the reduced red mud catalyst indicated the presence of acid and base sites (Figs. 4SD and 5SD). Ammonia TPD analysis indicated acid adsorption sites (peaks) at 120°C (physisorption), 280-320°C, 320-360°C, and 380-560°C for RRM (Fig. 4SD). CO_2 TPD analysis indicated the appearance of a peak at 500°C in the H_2 reduced red mud (Fig. 5SD).

Overall analysis of the characterization results suggest the resultant catalyst, H_2 reduced red mud, is a mixed metal oxide with both acid and base active sites. The N_2 adsorption/desorption isotherm exhibited significant H3 type hysteresis (Fig. 1SD) indicative of metal oxides and an irregular pore structure (e.g., $Fe_{0.2}Ce_{0.2}Al_{0.6}O_2$).[10] Similar to our results, doping of ferrites with a range of metals (Cr, Mn, Ni, Cu, Zn, and Ce) and subsequent H_2 reduction significantly increases surface area.[24] The acid sites (peaks) at 280-320°C, 320-360°C, and 380-560°C indicated by NH_3-TPD are consistent with a mixed metal oxide. CeZrOx and Fe_xCe_y-Al_zO_2 reportedly have NH_3 adsorption sites at 286-326°C and 100-400°C (a single broad peak), respectively.[10, 25] There is one clear CO_2-TPD peak for the H_2 reduced red mud at 500-

550°C, suggestive of a base adsorption site (Fig. 5SD). CeZrOx catalysts used in ketonization studies of acetic acid and 1-hydroxy-2-propane are reported to have three CO_2 adsorption sites – weak (27-227°C), intermediate (227-427°C), and strong (427-727°C) sites.[25] Although not clearly indicated in our XRD analysis, previous analysis indicate a range of mineral phases in red mud, including hematite (Fe_2O_3), goethite (FeO(OH)), anatase (TiO_2), boehmite (AlO(OH)) or gibbsite($Al(OH)_3$), mixed silicates, and calcite ($CaCO_3$).[15] And it is widely acknowledged that the composition of red mud is variable and dependent upon the source. Thus, the peak from 650-700°C in the CO_2-TPD is probably CO_2 evolved from the thermal decomposition of calcite. Calcite in red mud decomposes from 600-800°C via $CaCO_3 \rightarrow CaO + CO_2$, similar to our CO_2-TPD profile.[26]

3.2 Catalytic Ketonization Model Compounds

Our analysis of the fast pyrolysis oil (FPO) indicated high levels of acetic acid, formic acid, 1-hydroxy-2-propanone and levoglucosan with lower levels of furfural and 5-hydroxymethyl furfural (Table 2). These findings dictated our selection of model compounds, their defined concentrations, and our decision to use water extracted FPO. Given the complexity of FPO, a series of experiments were first performed on individual model compounds (4 wt. % each in water: acetic, formic, 1-hydroxy-2-propanone, and levoglucosan) and catalytically transformed using RRM in typically 0.5-1h runs. The feed and condensed products were analyzed via GC/MS, GC/FID and HPLC in an attempt to understand the reaction pathways for the individual model compounds.

Acetone was the primary product from acetic acid, clearly indicating the reduced red mud (RRM) catalyzed ketonization of acetic acid. Interestingly, the reaction rates for RRM were

similar to those reported for CeZrOx (Fig. 1C, D; 3-11 for CeZrOx vs. 8 mmol/g-cat/h for RRM), but our acetone selectivity (moles produced/moles converted) was lower (8-17% excluding formic acid vs. 40%).[25] In our work, levoglucosan reactivity was lower than the other compounds (3 vs. 6-11 mmol/g-cat/h), but severe plugging was not observed (Fig. 1D). Acetone, 1-hydroxy-2-propanone (acetol or 2HP) and formic acid were the primary products formed from levoglucosan (Table 1SD). Apparently, ketone (diketone and cyclicketone) formation from levoglucosan occurred via the intermediates acetic acid ($Y_{aa} = 0.47$), acetol ($Y_{2HP} = 0.124$), and formic acid ($Y_{fa} = 0.23$), since they were identified via GC/MS and HPLC in the products and their yields were higher than acetone (Fig. 1C and Table 1SD). Trace peaks of acetaldehyde, 2,3-butanedione,2-butanedione, cyclopentanone, 2-methyl-2-cyclopenten-1-one, furfural, and levoglucosenone were also observed (via GC/MS) from levoglucosan (Table 1SD). Individual conversion of acetol yielded acetone and 2-butanone at higher yields than acetic acid (Fig. 1A). Trace peaks of acetaldehyde, 2,5-hexanedione, 2,3-butanedione, 2,3-pentanedione, acetic acid, propanoic acid, 2-methyl-2-cyclopenten-1-one, and 3-methyl-2-cyclopenten-1-one were observed from acetol. Although formic acid conversion and reaction rates were significantly higher than the other compounds (Fig. 1A, D), only trace levels of acetone and methanol were observed, and interestingly acetic acid was formed from formic acid (Table 1SD). Space time conversions (STY) mirrored reaction rates and were reasonably high – 330 (acetic or AA), 452 (formic or FA), 355 (acetol or 2HP), and 372 (levoglucosan) g converted/L-cat/h.

The distribution of our primary and trace products for catalytic reaction of acetic acid, acetol, and levoglucosan (Table 1SD) suggest a ketonization pathway similar to one proposed using a ceria–zirconia (CeZrOx) mixed oxide catalyst.[25] These researchers indicated that acetol was converted to pyruvaldehyde and 1,2-propylene glycol via transfer hydrogenation.

Pyruvaldehyde is decarbonylated to acetic acid and formaldehyde or formic acid and acetaldehyde. Acetic acid can then undergo ketonization to form acetone, which can condense with pyruvaldehyde and then undergo hydrogenation to form a diketone (e.g., 2,5-hexanedione). Decomposition of formic acid to H_2 provides an internal hydrogen donor. The diketones can then undergo base-catalyzed intramolecular cyclization to form cyclic ketones (e.g., 3-methyl cyclopent-2-en-1-one). The formation of 2-butanone results from the dehydration of propylene glycol to form propanal, which undergoes carbonylation, hydrogenation, and dehydration.[25] Propanoic acid formation was theorized to occur via a disproportionation reaction and then undergo ketonization.[25] Consistent with this theory we observed acetic acid, acetone, and 2-butanone as primary products, and trace levels of propanoic acid, diketones and cyclic ketones from acetol using reduced red mud (Table 1SD). However, we did not observe pyruvaldehyde, propanal, propylene glycol, formaldehyde or formic acid formation (from acetol), all of which may have been below our detection limits or rapidly reacted under our conditions.

The primary and trace products formed from levoglucosan also suggest a ketonization pathway (Table 1SD). Acetic acid, acetol, and formic acid all are formed in high yields from levoglucosan, indicating that each of these products should enter the previously described pathways for acetic acid ketonization and acetol transfer hydrogenation via hydrogen generated from the decomposition of formic acid. The most noticeable differences, relative to acetol, were the formation of furfural and levoglucosenone, and higher levels of 2,3-butanedione (Table 1SD). The formation of levoglucosenone and furfural indicate a dehydration step catalyzed by acid sites in the RRM. A sulfonic acid functionalized resin, Amberlyst 70, has recently been demonstrated to catalyze the formation of these two compounds from levoglucosan in DMSO.[27] The formation of 2,3-pentanedione and 2,3-butanedione (diacetyl) could be explained by the

ketonization of lactic acid[28] and condensation of acetaldehyde or acetic and lactic acid to form acetoin (3-hydroxy-2-butanone) and subsequent dehydrogenation of acetoin to diacetyl.[25] A tentative reaction pathway for the conversion of acetic acid, acetol, and levoglucosan to identified products, based on our results and literature analysis, is presented in Figure 6SD. [25-29]

To better understand the interaction between reactants we next performed catalytic runs using model compound mixtures (acetic-formic, acetic-formic-acetol, acetic acid/2-methoxy phenol). Addition of formic acid, acetol (1-hydroxy-2-propanone), and 2-methoxy phenol (2MP) reduced acetone yield and the rate of acetic acid ketonization and conversion, yet the formic acid reaction rate was independent of the other compounds (Fig. 1E). It is interesting to note that the presence of 2MP reduced the acetic acid reaction rate and yield, yet the acetone selectivity was unaffected (Fig. 1C). At this point we believed the overall lower acetone yield in the mixture (Fig. 1C) was due to incomplete conversion of acetic acid and intermediates formed from acetol.

Thus, we performed a series of experiments where both the temperature and residence time was increased by lowering the liquid feed rate (1 to 0.5 ml/min) and increasing the catalyst mass (10, 15, and 20 g). Increasing contact time with the catalyst and increasing the reaction temperature increased the acetone and total ketone selectivity to 22% (Fig. 2). We note that ketone yield and selectivity was potentially higher, since 2 and 3-pentanone and 3-methyl-2-butanone were observed via GC/MS, yet standards were not available for quantification. Trace peaks of 3-methyl-2-pentanone, 3-hexanone, cyclopentanone, and 2 and 3-methylcyclopentanone were also observed. It is interesting to note that methanol and 2,3-butanedione formation were observed at the lower W/F ratio and disappeared at the highest W/F ratio.

3.3 Catalytic Ketonization of Water Extracted Fast Pyrolysis Oil

Given the positive results with model compounds and representative mixtures, we were prompted to investigate catalytic ketonization of water extracted fast pyrolysis (WE-FPO) oil in a continuous packed bed reactor (350°C, 5 g cat., 1 ml/min liq. feed, 100 ml/min N_2). Aqueous phase fractions typical of the type noted in Table 2 were used in these experiments. The inlet composition of this WE-FPO (UGA oil) consisted of acetic acid (37-48 g/L), formic acid (34-57 g/L), acetol (3-5 g/L), levoglucosan (50-129 g/L), furfural (0.4-2.25 g/L), 5-hydroxymethyl furfural or HMF (0-2.3 g/L), and 2-methoxy phenol (0.4-3 g/L), and methanol (0-4.9 g/L). Total conversion of organics in these feeds was low and the net conversion of acetol was negligible (Fig. 7SD). This was due to the fact that levoglucosan was converted to acetol and residence times were too low for complete acetol transformation. The higher WHSV (due to higher inlet molar rates) also contributed to the lower conversions and subsequent lower acetone/2-butanone selectivity. The catalytically treated, water extracted bio-oil, did have higher levels of long chain and cyclic ketones (in 3 out of 4 runs, 1-hydroxy-2-butanone, 2-butanedione, 2,3-butanedione, cyclopentanone, and cyclopentadione were observed) compared to the model compound results (Fig. 6SD). At this point it was felt that acetic acid and acetol (2HP) conversions, and ketone yields, could be increased by increasing the reaction temperature and catalyst mass.

Thus, a series of experiments were performed in which the reaction temperature and catalyst mass were increased. Since FPO composition can change, even if stored at 4°C, we performed complete analysis of the feedstock before use. The inlet consisted of acetic acid (47 g/L), formic acid (15 g/L), acetol (10 g/L), levoglucosan (44 g/L), furfural (1.2 g/L), HMF (0.75 g/L), 2-methoxy phenol (1.2 g/L), and methanol (0.8 g/L) and water extracted FPO was used as the feedstock. Holding the catalyst mass constant and increasing the reaction temperature clearly increased the conversion and measured reaction rate of oxygenates and levoglucosan in the water

extracted fast pyrolysis oil (WE-FPO). At a low temperature (350°C) there was no measureable net conversion of acetol (due its formation from levoglucosan), but net conversion of measured components approached >80% at 425°C (Fig. 3). Increasing the temperature resulted in an increase in the acetone selectivity (and yield-data not shown) and the total ketone yield (Σ acetone, 2-butanone, and butyrolactone) approached 22% (the total ketone yield was 19% - Fig. 3). It is interesting to the note that butyrolactone was observed, yet its selectivity and yield, as well as for 2-butanedione, declined with increasing temperature (Fig. 3).

Next a series of experiments were performed at 400°C with increasing amounts of catalysts. As the W/F ratio was increased from 1.4 to 4.2 h, conversions of acetic acid, formic, acetol and levoglucosan all approached 100% (Fig. 4). Acetone and 2-butanone yields increased slightly and selectivity remained relatively constant with increasing catalyst mass (Fig. 4). In addition to acetone and 2-butanone, a range of cyclic ketones were produced, potentially due to similar sequential condensation reactions demonstrated with our model compound mixtures. This was most apparent when performing a chromatogram and mass spectral overlay (via MS Chemstation and NIST 08 library and MS Search V.2 software). At the lower W/F ratio acetone was the primary product with smaller peaks of acetaldehyde, 2,3-butanedione, 2-butanone, 2-methyl-2-cyclopenten-1-one, butyrolactone and residual acetic acid and 1-hydroxy-2-propanone (Fig. 5). As the W/F ratio was increased, the acetaldehyde, 2,3-butanedione, butyrolactone, acetic acid, and 1-hydroxy-2-propanone peaks disappear. At the largest W/F ratio a series of new compounds are clearly formed including methanol, ethanol, 3-methyl-2-butanone, 2-pentanone, cyclopentanone, 2-methyl-cyclopentanone, 2-methyl-2-cyclopenten-1-one, and 3,4-dimethyl-2-cyclopenten-1-one (Fig. 5, MS match factors in Table 1SD). There have been limited studies on continuous catalytic ketonization of whole oil or water separated oil for comparison of our

results. Mansur et al. 2013 performed continuous ketonization of an aqueous phase generated from slow pyrolysis oil (cedar) using a ZrO_2-FeOx catalyst.[29] Similar to our results, acetol and carboxylic acids in the oil were converted to primarily acetone and 2-butanone with the highest yields (30 mol% based on carbon) occurring at a W/F of 4 h and 350°C.

3.4 Catalyst Surface Properties

After reaction, catalysts were recovered, washed, dried and characterized to determine the formation of coke. Surface area and pore size analysis, after rinsing with a solvent mixture, indicated the formation of coke, primarily when using the water extracted (WE) commercial oil. As noted in Table 3 and Figure 8SD, the largest increase in tar (based on an increase in mass), an approximate 20-40% increase in tar, was observed when upgrading the WE-oil, compared to 0-5% for formic, acetic, acetic acid/1-hydroxy-2-propanone, acetic acid/2-methoxy phenol, and levoglucosan. Corroborating these results, pore size and air-TGA analysis clearly indicated a significant reduction in pore volume for the WE-oil's and significant mass loss from 200-500°C upon oxidation (Figures 9SD and 10SD). In the TGA analysis (after solvent washing and drying) of the WE-oil catalyst sample there was a 13% mass loss, with a significant fraction of the loss occurring from 200 to 500°C. This compares to an 8% loss for the control (fresh RRM catalyst) and 8% or less for all of the other reacted samples (Fig. 9SD). As previously noted we believe the mass loss from 600-650°C in the TGA studies was due to CO_2 loss due to calcite decomposition. This peak in mass loss (600-650°C) was observed in every reacted catalyst sample, as well as the fresh H_2 reduced red mud (RRM) (Fig. 10SD). The one exception in these trends, was the small change in surface area and pore volume and little mass loss in the TGA analysis for the catalyst reacted with formic acid (Figs. 8SD, 9SD, and 10SD).

4. Conclusions

Phase separation of fast pyrolysis oil into an aqueous phase and subsequent treatment using a multi-functional catalyst capable of performing cascading transfer hydrogenations, ketonization, and condensation reactions significantly reduced acid levels and generated liquid fuel intermediates. This approach could also prove complementary with previously demonstrated catalytic treatments of the bio-oil non-polar phase. The reduced red mud acts catalytically in a manner similar to a mixed metal oxide, since it has both acid/base sites and redox properties. Increasing the catalyst mass to feed rate ratio (W/F) increased the yield of acetone/2-butanone (22%) and cyclic ketones from a mixture of acetic, formic, and acetol (4% each) and water extracted fast pyrolysis oil (15-20 mol% ketones, W/F 1.4-4 h, 400-425°C). The highest space time yields (STY) approached 60 g (acetone+2-butanone)/L-cat/h for the model mixture and 120 g/L-cat/h for the commercial oil indicating the feasibility of synthesizing an inexpensive catalyst from red mud suitable for "continuous" upgrading.

5. Acknowledgements

The authors graciously thank Joby Miller, Richard Spier, and Andrew Smola for their invaluable contributions of time and effort in analyzing materials and gaseous compositions. The financial support for this study provided by a SunGrant and DOE (DEFG3608GO8814: Biorefining and Carbon Cycling Program).

6. References

1. G.W. Huber, Breaking the Chemical and Engineering Barriers to Lignocellulosic Biofuels: Next Generation Hydrocarbon Biorefineries. Based on the June 25-26, 2007 Workshop, Washington, D.C., Sponsored by NSF, DOE, and ACS. p.1-179.

2. T. P. Vispute, H. Zhang, A. Sanna, R. Xiao, G. W. Huber, *Science,* 2010, **330**, 1222-1227.

3. J. P. Diebold, NREL/SR-570-27613, 2000.

4. J. P. Diebold, *Energy Fuels*, 1997, **11**, 1081-1091.

5. F. Mahfud, I. Melián-Cabrera, R. Manurung, H. Heeres, *Process Saf. Environ.*2007, **85**, 466-472.

6. A. G. Gayubo, A. T. Aguayo, A. Atutxa, J. Bilbao, *Chem. Technol. Biotechnol.,* 2005, **80**, 1244–1251.

7. A. G. Gayubo, A. T. Aguayo, A. Atutxa, R. Prieto, J. Bilbao, *Energy Fuels,* 2004, 18, 1640-1647.

8. R. Hilten, B. Bibens, J. Kastner, K.C. Das, *Energy Fuels*, 2010, **24**, 673–682.

9. M. Glifiski, J. Kijefiski, A. Jakubowski, *Appl. Catal. A: Gen.* 1995, **128**, 209-217.

10. M. A. Jackson, *Energy Fuels*, 2013, **27**, 3936.

11. E. Karimi, A. Gomez, S.W. Kycia, M. Schlaf. *Energy Fuels*, 24, 2747-2757, 2010.

12. E. Karimi, I. F. Teixeira, L. P. Ribeiro, A. Gomez, R. M. Lago, G. Penner, S. W. Kycia, M. Schlaf, *Catal. Toda*y, 2012, **190**, 73-88.

13. E. Karimi, I. F. Teixeira, A. Gomez, E. de Resende, C. Gissane, J. Leitch, V. Jollet, I. Aigner, F. Berruti, C. Briens, P. Fransham, B.Hoff, N. Schrier, R.M. Lago, S.W. Kycia, R. Heck, M. Schlaf. *Appl. Catal. B: Environ.* (2014), 145, 187-196.

14. E. Karimi, C. Briens, F. Berruti, S. Moloodi, T. Tzanetakis, M.J. Thomson, M. Schlaf. *Energy Fuels*. 2010, 24, 6586-6600.

15. S. Sushil, V. S. Batra, *Appl. Catal. B: Environ.* 2008, **81**, 64–77.

16. S. Sushil, V. S. Batra, *Journal of Solid Waste Technology and Management*, 2011, **37**, 188-196.

17. S. Eijsbouts, G. H. Anderson, J.A. Bergwerff, S. Jacobi, *Appl. Catal. A: Gen.* 2013 **458**, 169– 182.

18. J. X. Fu, C. Zhang, W. S. Hwang, Y. T. Liau, Y. T. Lin, *Int. J. Greenh.Gas Con.* 2012, **8**, 143–149.

19. S. Hosokai, K. Matsui, N. Okinaka, K. Ohno, M. Shimizu, T. Akiyama, *Energy Fuels,* 2012, **26**, 7274−7279.

20. A. H. Zacher, M. V. Olarte, D. M. Santosa, D. C. Elliott, S. B. Jones, *Green Chem.,* 2014, **16**, 491.

21. C. Zhao, J.A. Lercher, *Angew. Chem. Int. Ed.* 2012, 51, 5935-5940.

22. N. M. Bennett, S.S. Helle, S.J.B. Duff, *Bioresour. Technol.* 2009, **100**, 6059–6063.

23. C. R. Vitasari, G.W. Meindersma, A. B. Haan, *Bioresour. Technol.* 2011, **102**, 7204–7210.

24. A. Khan, P. G. Smirniotis, *J. Mol. Cat. A- Chem.* 2008, **280**, 43–51.

25. S. H. Hakim, B. H. Shanks, J. A. Dumesic, *Appl. Catal. B: Environ.* 2013, **142–143**, 368– 376.

26. C. Wu, D. Y. Liu, *Journal of Nanomaterials*, 2012, **2012**, 1-6.

27. X. Hu, L. Wu, Y. Wang, D. Mourant, C. Lievens, R. Gunawan, C. Z. Li, *Green Chem*., 2012, **14**, 3087.

28. P. Mäki-Arvela, I. L. Simakova, T. Salmi, D. Y. Murzin, *Chem. Rev.*, 2014, **114**, 1909−1971.

29. D. Mansur, T. Yoshikawa, K. Norinaga, J. Hayashi, T.T. Takao, Masuda, *Fuel*, 2013, **103**, 130-134.

Table 1: Compositional analysis of red mud and H_2 reduced red mud catalyst (RRM).

Table 2: HPLC and GC/MS analysis of aqueous and non-aqueous phase fast pyrolysis oil (generated from Southern Pine and a commercially produced oil).

Table 3: Physical properties of catalyst after ketonization of model compounds and water extracted FPO.

Figure 1: Continuous catalytic ketonization of model compounds and mixtures (4 wt% each) using reduced red mud at 350°C, 1 atm, 5 g catalyst, and a WHSV of 0.48 h^{-1} ($g_{reactant\ fed}$/g-cat/h). Note-2HP is acetol, aa is acetic, fa is formic, X is conversion, r is reaction rate, and 2-MP is 2-methoxyphenol at 1 wt%. A – Conversion for model compounds, B – Effect of other compounds on acetate conversion, C – Yield and selectivity for model compounds and mixtures, D – Reaction rate for model compounds, and E – Effect of other compounds on acetic acid reaction rate.

Figure 2: Effect of lower liquid feed rate and increased catalyst mass on catalytic ketonization of an aqueous mixture containing acetic, formic, and acetol or 2HP (4 wt.% each) using reduced red

mud at 350°C (open symbols) and 400°C (closed symbols) and 1 atm (5, 10, 15 and 20 g of catalyst). The catalyst mass/molar rate ratio (W/F) and space time yield (STY) is for all three compounds or a total.

Figure 3: Effect of temperature on the catalytic ketonization of water extracted fast pyrolysis oil (UGA oil) at a liquid rate of 1 ml/min, 5 g catalyst, 1 atm, resulting in a WHSV of 0.72 g oil/g-cat/h, or W/F = 1.38 h. The arrow indicates the lack of acetol or 1-hydroxy-2-propanone (2HP). CO indicates commercial fast pyrolysis oil.

Figure 4: Effect of catalyst mass on the catalytic ketonization of water extracted fast pyrolysis oil at 400°C and a liquid rate of 1 ml/min at 1 atm.

Figure 5: Effect of catalyst mass on intermediate and product formation during catalytic ketonization of water extracted fast pyrolysis oil using reduced red mud (400°C, 1 atm, 100 ml/min N_2 . 1-acetaldehyde; 2-acetone; 3-2,3-butandione; 4-2-butanone; 5-acetic acid; 6-1-hydroxy-2-propanone; IS, internal standard hexanol; 7-2-methyl-2-cyclopenten-1-one; 8-butyrolactone; 9-methanol; 10-3,4-dimethyl-2-cyclopenten-1-one; 11-ethanol; 12-3-methyl-2-butanone; 13-2-pentanone; 14-cyclopentaone; 15-2-methyl-cyclopentanone.

Table 1: Compositional analysis of red mud and H_2 reduced red mud catalyst (RRM).

Properties	Red Mud	RRM
Al, % (dry basis)	14.4	16.6
Ca, %	4.4	5.2
Fe, %	22.6	23.9
Na, %	14.5	15.9
Si, %	8.6	9.3
Ti, %	4.4	4.8
K,%	1.8	1.7
Mg,%	0.4	0.3
P,%	0.2	0.2
V,%	0.3	0.2
Surface Area (m^2/g)	13.3	30.7
Pore Volume (cm^3/g)	0.0091	0.024
Average Pore Size (radius), Å	13.58	15.63

Table 2: HPLC and GC/MS analysis of aqueous and non-aqueous phase fast pyrolysis oil (generated from Southern Pine and a commercially produced oil).

Oil	Levoglucosan (g/L)	Acetol (g/L)	Formate (g/L)	Acetate (g/L)	5-HMF (g/L)	Furfural (g/L)	Water (%)
UGA-ILC (aq)	75-90	3.2	50-65	30-37	1.5-1.7	0.8-1.0	Spray
UGA-FPO (aq)	74	5.0	57	37	2.25	1.5	50
UGA-FPO (oil)	130	15-17	80	72	3.0	2.5	20
Commercial Oil (aq)	51	10.3	34	50	1.0	2.4	50
Commercial Oil (oil)	57	36	NP	58	1.1	6.4	20

ILC – In-line condensation; NP-Not Performed; FPO-Fast Pyrolysis Oil
Acetol is 1-hydroxy-2-propanone

Table 3: Physical properties of catalyst after ketonization of model compounds and water extracted FPO.

Reactant	Catalyst	Surface Area (m^2/g)	Average Pore Size (Å)	Average Pore Volume (cm^3/g)	% Increase in Tar[a]	% Coke TGA[b]
None	Granulated Red Mud	13.3	13.58	0.0091	-	
None	H_2 Reduced (RRM)	30.7	15.63	0.024	-	
Acetic Acid	RRM-Reacted	20.8	15.3	0.016	4.0	0.0
Formic Acid	RRM-Reacted	32.5	15.5	0.025	1.5	0.0
Acetol	RRM-Reacted	26.1	15.4	0.02	4.0	0.0
Acetic, Formic	RRM-Reacted	24.8	16.1	0.02	4.0	0.0
Acetic, Formic, Acetol	RRM-Reacted	16.7	16.3	0.014	2.0	0.0
Acetic and 2-MP	RRM-Reacted	16.5	16	0.013	0.0	0.0
Levoglucosan	RRM-Reacted	27.3	14.6	0.0198	6.0	1.02
Commercial Oil Aq. Phase	RRM-Reacted	15.1	15.37	0.0116	18.0	4.63
UGA FPO Aq. Phase	RRM-Reacted	12.4	15.30	0.0095	38.0	0.0

[a], based on mass loss after rinsing with solvent

[b], based on the mass loss during TGA analysis (in air), after solvent washing and with mass loss from fresh catalyst (RRM) subtracted

2MP – 2-methoxy phenol

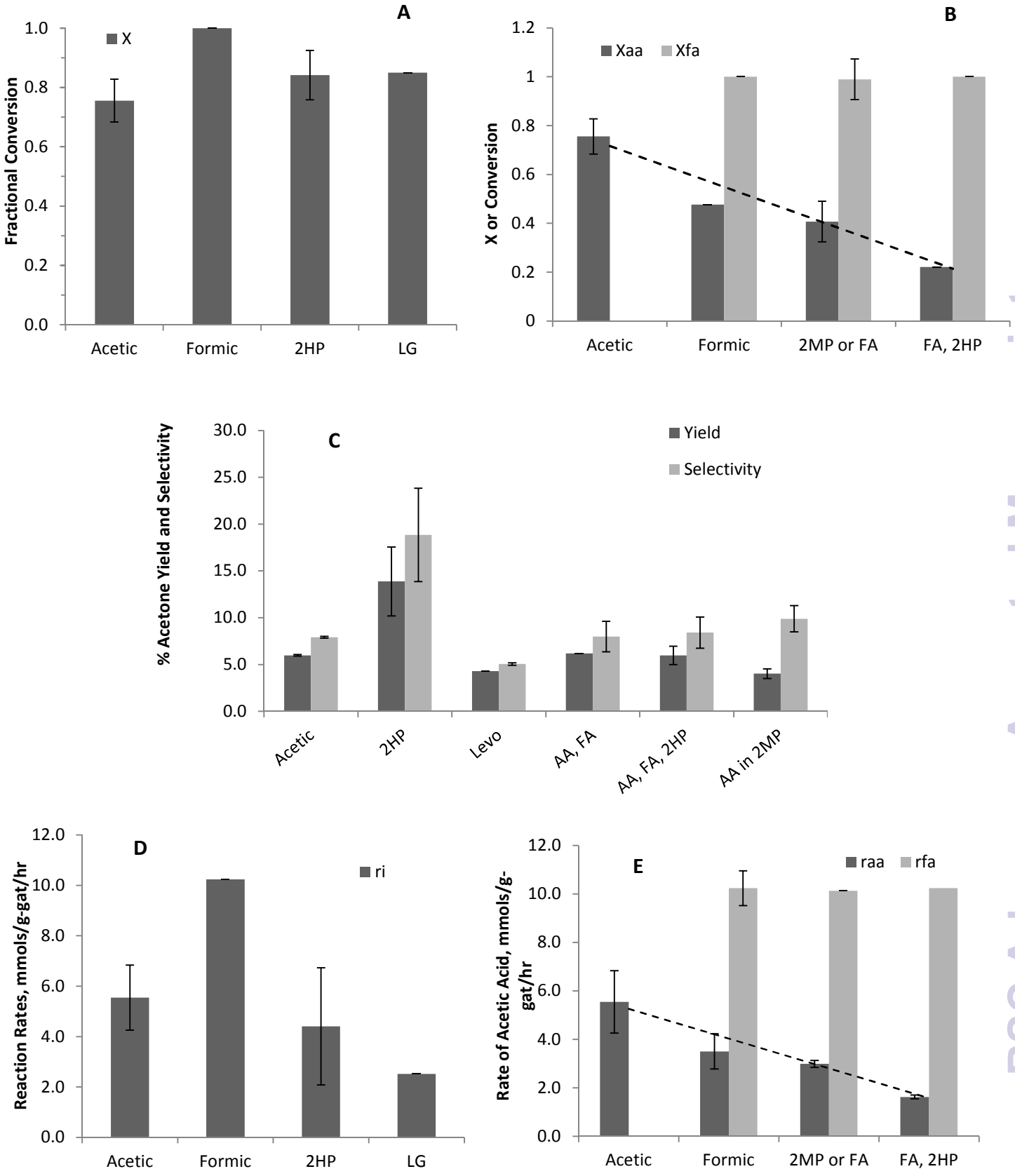

Figure 1: Continuous catalytic ketonization of model compounds and mixtures (4 wt% each) using reduced red mud at 350°C, 1 atm, 5 g catalyst, and a WHSV of 0.48 h^{-1} ($g_{reactant\ fed}$/g-cat/h). Note-2HP is acetol, aa is acetic, fa is formic, X is conversion, r is reaction rate, and 2-MP is 2-methoxyphenol at 1 wt%. A – Conversion for model compounds, B – Effect of other compounds on acetate conversion, C – Yield and selectivity for model compounds and mixtures, D – Reaction rate for model compounds, and E – Effect of other compounds on acetic acid reaction rate.

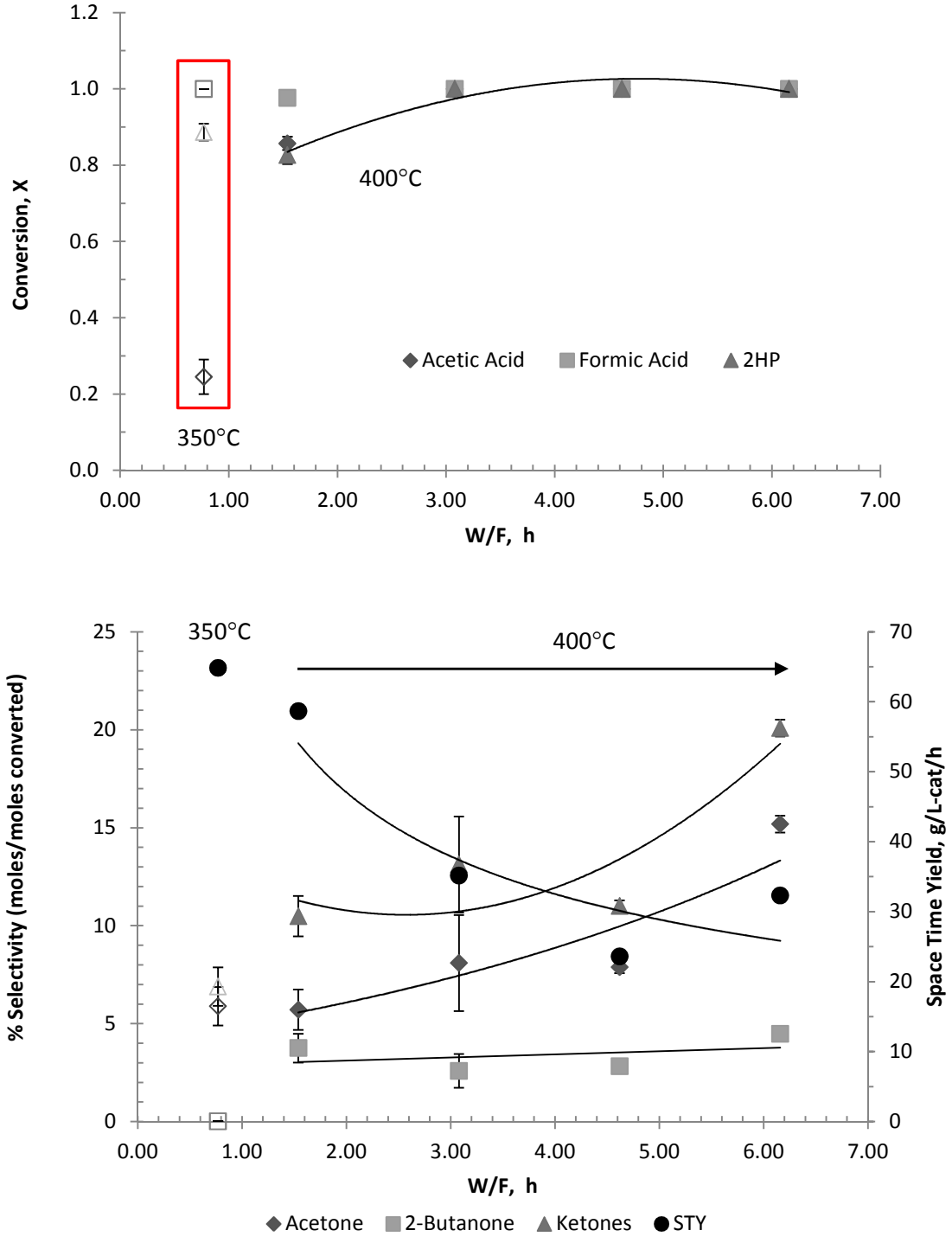

Figure 2: Effect of lower liquid feed rate and increased catalyst mass on catalytic ketonization of an aqueous mixture containing acetic, formic, and acetol or 2HP (4 wt.% each) using reduced red mud at 350°C (open symbols) and 400°C (closed symbols) and 1 atm (5, 10, 15 and 20 g of catalyst). The catalyst mass/molar rate ratio (W/F) and STY is for all three compounds or a total.

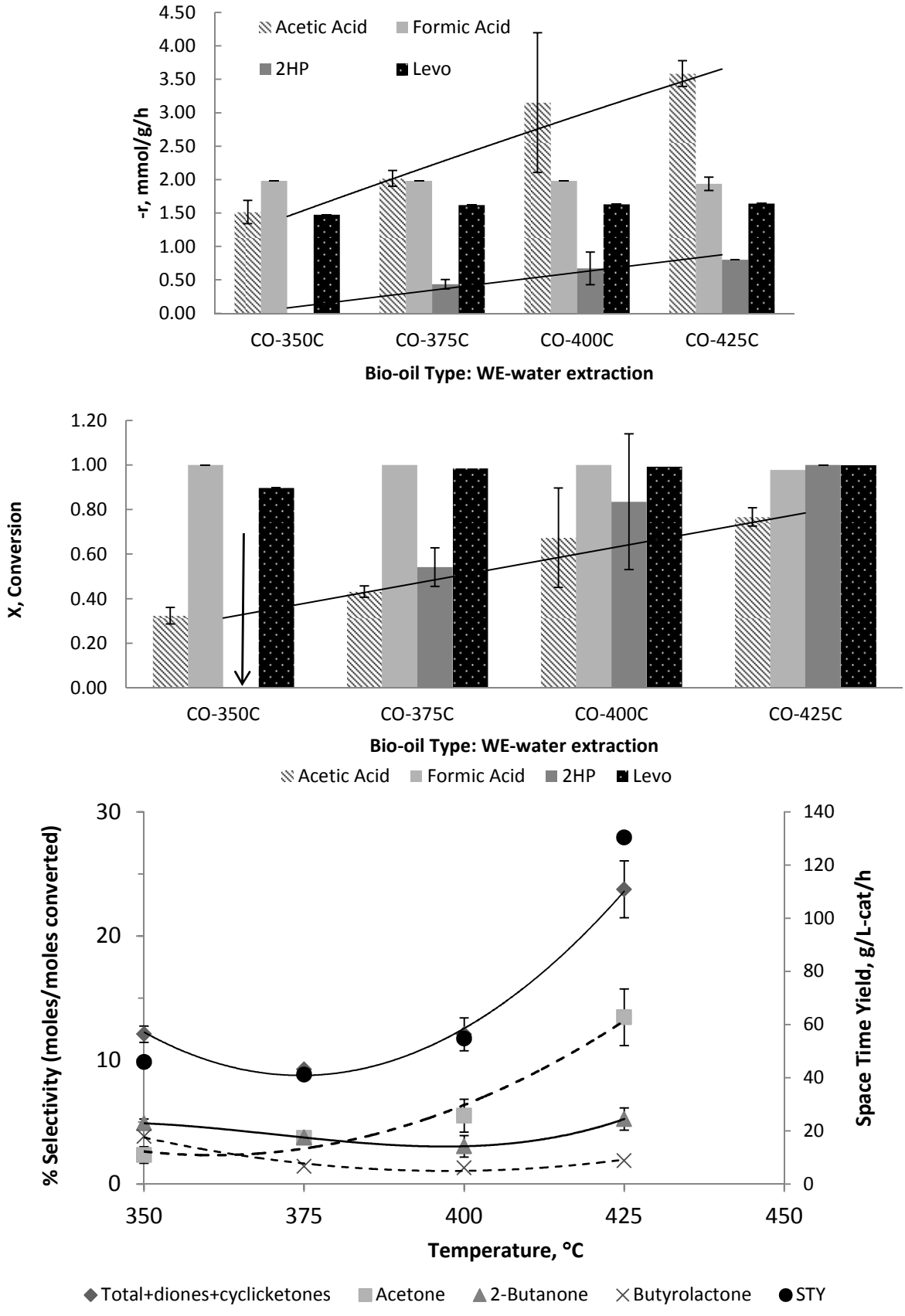

Figure 3: Effect of temperature on the catalytic ketonization of water extracted fast pyrolysis oil (UGA oil) at a liquid rate of 1 ml/min, 5 g cat. at 1 atm, resulting in a WHSV of 0.72 g oil/g-cat/h, or W/F = 1.38 h. The arrow indicates the lack of acetol or 1-hydroxy-2-propanone (2HP). CO indicates commercial fast pyrolysis oil and WE is water extraction.

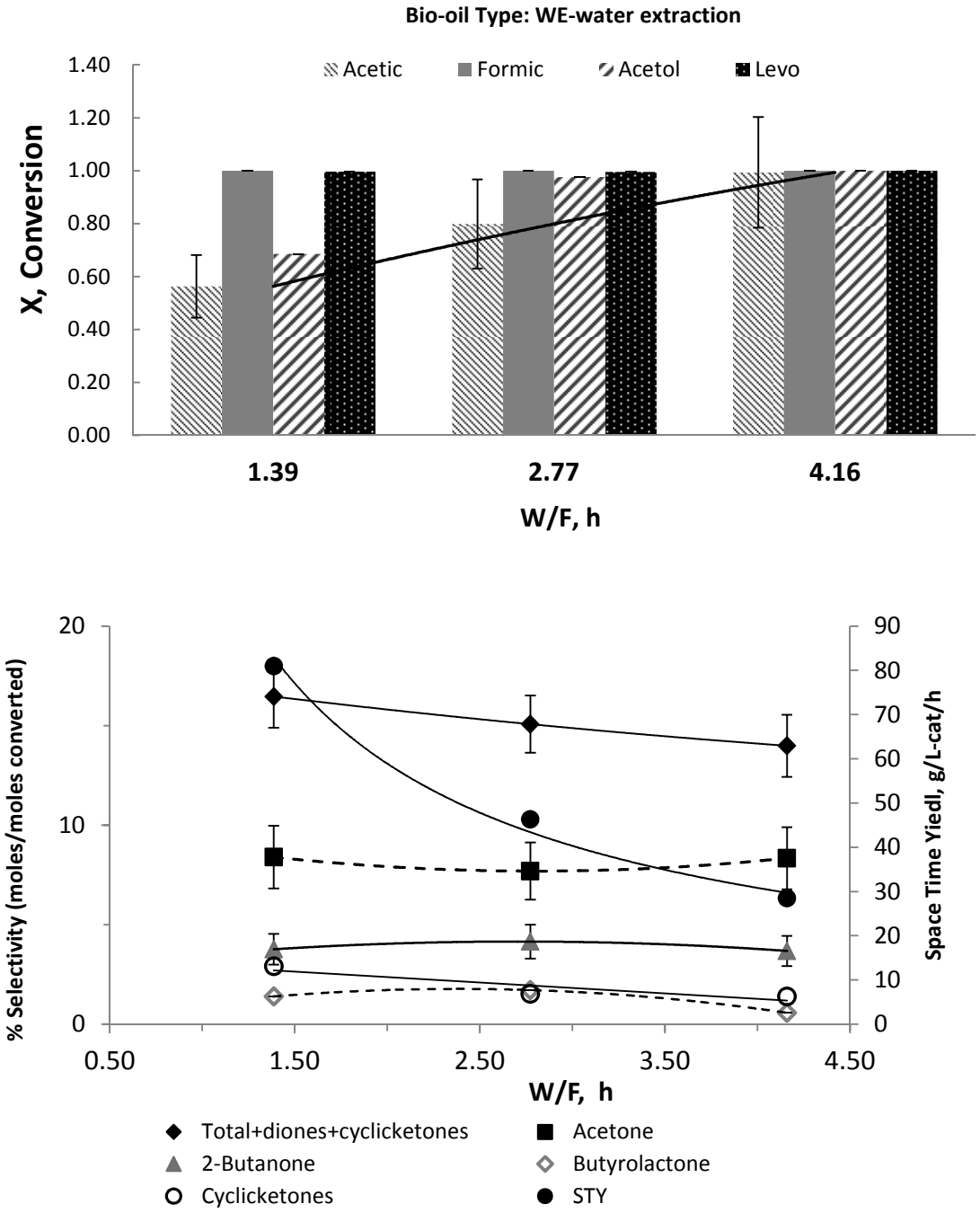

Figure 4: Effect of catalyst mass (RRM) on the catalytic ketonization of water extracted fast pyrolysis oil at 400°C and a liquid rate of 1 ml/min at 1 atm.

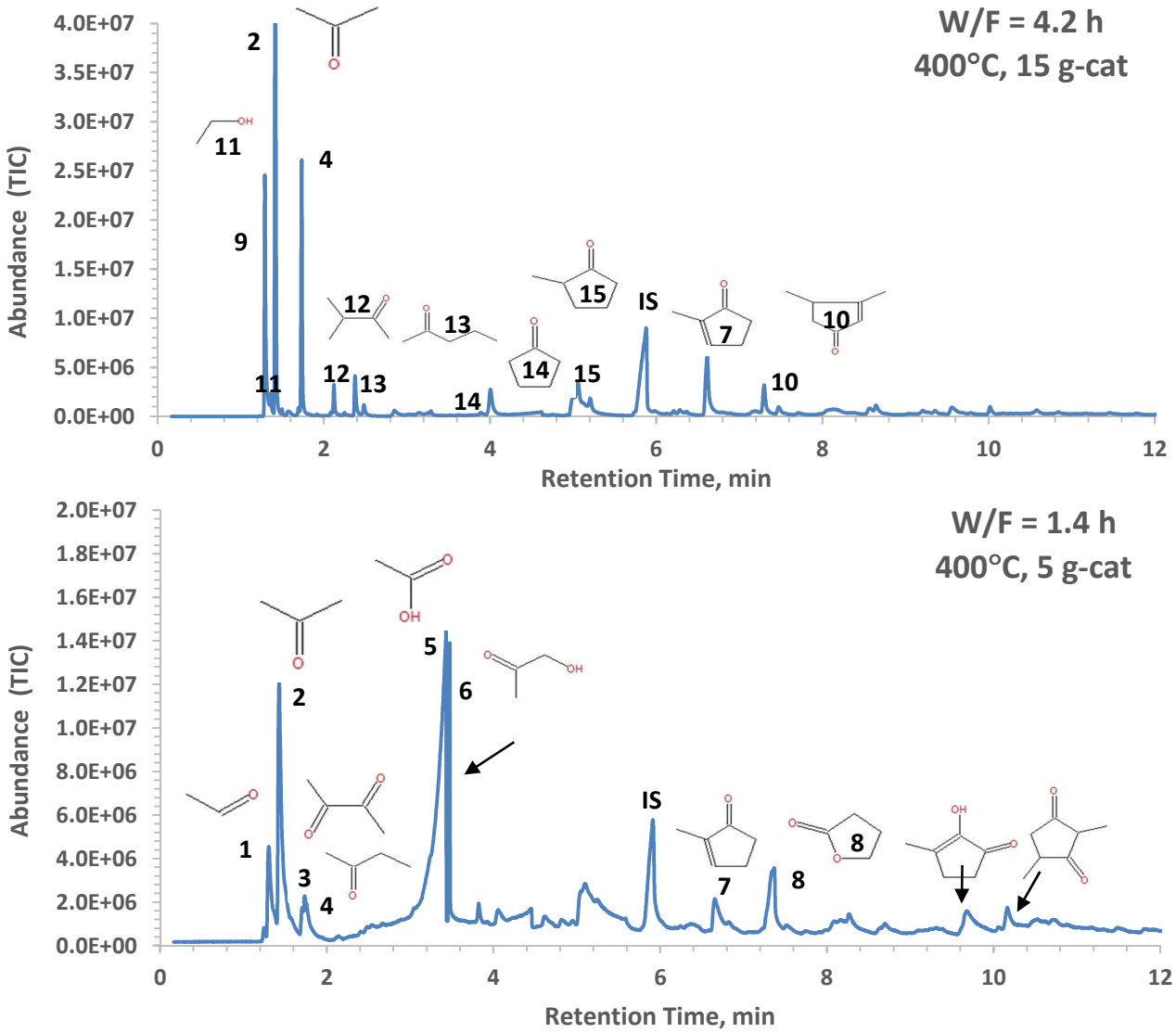

Figure 5: Effect of catalyst mass on intermediate and product formation during catalytic ketonization of water extracted fast pyrolysis oil using reduced red mud (400°C, 1 atm, 100 ml/min N_2 . 1-acetaldehyde; 2-acetone; 3-2,3-butandione; 4-2-butanone; 5-acetic acid; 6-1-hydroxy-2-propanone (acetol); IS, internal standard hexanol; 7-2-methyl-2-cyclopenten-1-one; 8-butyrolactone; 9-methanol; 10-3,4-dimethyl-2-cyclopenten-1-one; 11-ethanol; 12-3-methyl-2-butanone; 13-2-pentanone; 14-cyclopentanone; 15-2-methyl-cyclopentanone.